



Prognostic Value and Oncogenic Effects of Ubiquitin-Specific Protease 43 in Lung Squamous Cell Carcinoma

Qingchao Sun,¹ Haiping Zhang,¹ Liang Zong,¹ Ainiwaer Julaiti,¹ Xiaoliang Jing¹ and Liwei Zhang¹

¹Department of Thoracic Surgery, The First Affiliated Hospital of Xinjiang Medical University, Xinjiang, China

Dysregulated expression of ubiquitin-specific protease 43 (USP43) has been recently discovered in malignancies. This study aimed to investigate the expression pattern of USP43 protein in lung squamous cell carcinoma (LUSC) and to explore its correlation with patients' clinicopathological characteristics as well as clinical outcomes. Expression of USP43 protein was determined by immunohistochemistry staining in a retrospective cohort containing 157 LUSC cases who underwent curative surgery in our hospital. Accordingly, USP43 protein was positively correlated with tumor size, depth of invasion, and lymph node metastasis. Patients with increased USP43 expression or positive lymph nodes exhibited a poorer overall survival. In addition, cellular assays elucidated that USP43 can promote LUSC growth and invasion. Taken together, our study demonstrated that USP43 may act as a proto-oncogene, which could be a promising biomarker and therapeutic target in the survival prediction and treatment of LUSC.

Keywords: invasion; lung squamous cell carcinoma; migration; proliferation; ubiquitin-specific protease 43
Tohoku J. Exp. Med., 2022 June, 257 (2), 135-145.
doi: 10.1620/tjem.2022.J008

Introduction

Lung cancer is one of the most common human malignancies and is the leading cause of cancer-related mortality worldwide. Lung cancer is comprised of three major subtypes, including lung squamous cell carcinoma (LUSC), lung adenocarcinoma (LUAD), and large cell lung carcinoma (LCLC) (Zhang et al. 2020). Among them, LUSC is the most common subtype, which results in approximately 400,000 deaths per year (Siegel et al. 2020). LUSC is characterized with high molecular complexity and most LUSC patients were diagnosed with advanced stages (Miller et al. 2016). Therefore, although great progress has been made, treatment of LUSC remains unsatisfied considering its high recurrence rate and poor prognosis (Zhang et al. 2018b). Efficient prognostic prediction of LUSC is critical to improve the survival rate and follow-up of LUSC cases. It is urgent to identify molecular biomarkers to help predict LUSC prognosis and direct novel therapeutic development (Zhang et al. 2017; Zou et al. 2019; Yan et al. 2021; Chen et al. 2021a, 2022).

Ubiquitination and phosphorylation perhaps represent the two most important post-translational protein modifica-

tions, especially in malignancies (Tang et al. 2018; Liu et al. 2019, 2021; Wang and Wang 2021). More and more studies suggest that ubiquitin plays a critical role in carcinogenesis and cancer progression (Liu et al. 2016; Gallo et al. 2017). Ubiquitin-specific protease (USP) family is a class of enzymes with protein deubiquitinating activity, comprising the majority of protein deubiquitinating diversity within mammalian cells (Pal and Donato 2014). USPs members are also emerging as prognostic factors and therapeutic targets in many diseases, including cancers (Young et al. 2019). However, USPs may play oncogenic or anti-tumor roles in different cancers. For example, USP14 was reported as an oncogene in several cancer types (Tian et al. 2014), while USP33 act as a tumor suppressor (Li et al. 2013).

Of note, even the same USP protein can have multiple effects in tumor. For example, USP24 was reported to suppress tumor cell proliferation but can also enhance tumor metastasis (Wang et al. 2017, 2018). As a novel identified USP member, the function of USP43 is largely unknown. Its role in cancers was firstly reported by Lin et al. (2017), who showed that USP43 promotes tumorigenesis through regulating cell cycle and EMT in breast cancer. Later,

Received November 19, 2021; revised and accepted December 20, 2021; J-STAGE Advance online publication March 24, 2022
Correspondence: Liwei Zhang, 137 Liyushan South Road, Xinshi District, Urumqi, Xinjiang 830054, China.
e-mail: z71893914@163.com

©2022 Tohoku University Medical Press. This is an open-access article distributed under the terms of the Creative Commons Attribution-NonCommercial-NoDerivatives 4.0 International License (CC-BY-NC-ND 4.0). Anyone may download, reuse, copy, reprint, or distribute the article without modifications or adaptations for non-profit purposes if they cite the original authors and source properly.
<https://creativecommons.org/licenses/by-nc-nd/4.0/>

USP43 was reported to promote the proliferation, migration, and invasion of colorectal cancer cells through overexpression and knockdown treatments (Ye et al. 2021). A recent RNA-sequencing study also revealed an increased USP43 in osteosarcoma cells, however, its correlation with osteosarcoma prognosis was not observed (Lavaud et al. 2021). Here we aimed to explore the expression of USP43 in LUSC tissues and test its clinical significance. Meanwhile, we investigated the tumor-related roles of USP43 in LUSC via cellular experiments.

Methods

Patients' information

A cohort of 157 LUSC patients was retrospectively enrolled from our hospital who underwent surgical resec-

tion from May 2009 to May 2012. None of the cases accepted preoperative chemotherapy treatment. All pathological diagnoses and staging were verified by the Department of Pathology according to the American Joint Committee on Cancer (AJCC) staging system. All the cases were treated with curative R0 resection; therefore, all resection margins were negative. Patients' basic information such as sex and age were retrieved. In brief, our cohort was comprised of 76 female patients and 81 male patients. There were 54 cases with age younger than 65-years-old. The clinicopathological characteristics, including tumor differentiation grade, tumor site, tumor laterality, tumor size in diameter, T stage, N stage and postoperative adjuvant therapy were all included in our statistical analyses (Table 1). In detail, 66 cases showed poor pathological differentiation,

Table 1. Correlations between USP43 expression and clinicopathological characteristics of 157 lung squamous cell carcinoma patients.

Variables	Cases (n = 157)	USP43 expression		P value
		Low (n = 81)	High (n = 76)	
Sex				0.801
Females	76	40	36	
Males	81	41	40	
Age				0.336
< 65 years	54	25	29	
≥ 65 years	103	56	47	
Differentiation grade				0.529
Well	19	12	7	
Moderate	72	35	37	
Poor	66	34	32	
Tumor site				0.892
Upper lung	100	52	48	
Middle/Lower lung	57	29	28	
Laterality				0.720
Left lung	70	35	35	
Right lung	87	46	41	
Tumor size				0.020*
< 3.0 cm	75	46	29	
≥ 3.0 cm	82	35	47	
T stage				< 0.001*
T1	52	34	18	
T2	67	39	28	
T3	31	7	24	
T4	7	1	6	
N stage				0.006*
N0	113	62	51	
N1	19	13	6	
N2	25	6	19	
Adjuvant therapy				0.022*
Rejected or unknown	97	57	40	
Accepted	60	24	36	

*Statistically significant by Chi-square test.
USP43, ubiquitin specific peptidase 43.

72 cases showed moderate differentiation, and the other 19 cases showed well differentiation. Among the 157 patients, 100 cases showed upper lung tumor location, while the other 57 cases showed middle or lower lung tumor location. Among them, 70 cases showed left lung tumor location, and the other 87 cases showed right lung tumor location. As for the tumor size, 75 cases were less than 5.0 cm in tumor diameter, and the other 82 cases were larger. According to the invasion depth, 52 cases were staged as T1 stage, 67 cases as stage T2, 31 cases as stage T3, and the other 7 cases as stage T4. Similarly, 113 cases were classified as N0 stage, 19 cases with N1 stage, while the other 25 cases with N2 stage. After surgical treatment, 60 cases accepted adjuvant therapy, while the other 97 cases were absent of adjuvant therapy. Besides the above patients enrolled from our medical center, we also retrieved the survival data of gastric cancer patients from TCGA database (<https://www.cancer.gov/tcga>).

Immunohistochemically (IHC) staining and IHC evaluation

All the 157 paired tissue sections from formalin-fixed paraffin-embedded blocks were deparaffinized, rehydrated, and then incubated in a pH 7.8 Tris-EDTA-citrate buffer at 121°C for 20 min for antigen retrieval. Primary antibody against USP43 (1:150 dilution) (#AP14283b, Abcepta, Australia) was incubated overnight at 4°C. Then slides were incubated with secondary antibody for 30 min at room temperature (Chen et al. 2021b).

Staining results were evaluated independently by two pathologists who were blinded to patients' characteristics. USP43 mainly localized in the cytoplasm of LUSC tissues. According to the cytoplasm staining, staining intensity was scored as negative staining (0), weak staining (1), moderate staining (2) or strong staining (3). At the same time, the percentage of stained cells was also scored: 0-25% positive cells (1), 26-50% positive cells (2), 51-75% positive cells (3), or 76-100% positive cells (4). The total immunoreactivity score was calculated by multiplication of these two scores above, ranging 0-12. According to the median staining score, patients were sub-grouped into two groups, the low-USP43 group (n = 81) and high-USP43 group (n = 76).

Cell lines and transfection

The human LUSC cell lines (NCI-H520 and NCI-H1703) and HEK293T cells were obtained from the Cell Bank of Chinese Academy of Sciences, Shanghai Branch. All the three cell lines were cultured in Dulbecco's modified Eagle's medium (DMEM) with 10% fetal bovine serum in 5% CO₂ and 90% humidity at 37°C.

The USP43 short hairpin RNA (shRNA) vector (shUSP43#1, shUSP43#2) and its negative control (scrambled shRNA) were synthesized by Genechem CO., Ltd. (Shanghai, China) as reported by others (He et al. 2018). Briefly, the recombinant constructs in pLKO.1 vectors, as well as assistant vectors psPAX2 and pMD2.G, were co-transfected into HEK293T cells. After culturing for 48 h,

the viral supernatants were collected, filtered, and concentrated, and were used to infect the NCI-H520 and NCI-H1703 cells, respectively. After infection, cells were selected with puromycin (#P9620, Sigma Aldrich, St. Louis, MO, USA) at 2.0 µg/ml concentration and maintained in 0.5 µg/ml puromycin during cell culture.

Western blot analysis

Cultured cells were lysed in radio-immunoprecipitation assay (RIPA) buffer (containing 1% phenylmethylsulfonyl fluoride) (#G2033, Servicebio, Wuhan, China) for extraction of total protein. BCA protein Assay kit (#23225, Thermo Fisher Scientific, Pittsburg, PA, USA) was applied to quantify the protein concentration. The protein samples (20 µg) were loaded on 10% SDS-PAGE and transferred to polyvinylidene difluoride (PVDF) membranes (#1620177, Bio-Rad, Hercules, CA, USA) which were blocked in 5% non-fat milk at room temperature for 1 h. Then primary antibodies (all 1:1,000 dilutions) were used to incubate with the PVDF membranes overnight. The primary antibodies for western blot included anti-USP43 (#AP14283b, Abcepta), anti-cyclin-dependent kinase 1 (CDK1) (#ab18, Abcam, Boston, MA, USA), anti-vimentin (#sc-6260, Santa Cruz Biotechnology, Dallas, Texas, USA), anti-snail (#sc-271977, Santa Cruz Biotechnology), and anti-GAPDH (#sc-47724, Santa Cruz Biotechnology). After then, secondary antibodies conjugated with horseradish peroxidase were used to incubate the membranes for another 1 h at room temperature. Finally, protein expression levels were visualized by ECL detection system (Zhang et al. 2018a). Experiments were repeated for three independent times.

Cell proliferation assay

Cell viability was monitored by Cell Count Kit 8 (#CK-04, Dojindo Molecular Technologies, Tokyo, Japan) according to the manufacturer's protocol. Briefly, infected LUSC cells were counted and seeded onto 96-well cell culture plates at a density of 2,000 cells per well. Proliferation rates were then measured by absorbance of 450 nm at 0, 1, 2, 3, and 4 days according to the standard procedure. Experiments were repeated for three independent times.

Transwell assay

Cell migration and invasion assays were performed with transwell chambers (#3464, Corning Biocoat, Corning, NY, USA). For the migration assay, cells were seeded into the upper chamber and incubated in FBS-free medium. The bottom chamber was filled with 20% FBS-containing medium. Following culture for 24 h, cells were fixed by paraformaldehyde and dye by crystal violet. Examination and counting of the cells were conducted under a microscope (Xu et al. 2018). The procedure of invasion assays was same to migration assays except that the chambers were pre-coated with Matrigel (0.5 mg/ml; #354234, Corning Biocoat). Experiments were repeated for three independent times.

Statistical analyses

Overall survival (OS) time was defined as the months from surgery date to the date of death or the last follow-up. Patients that survived less than 2 months after surgical resection were excluded to minimize perioperative death. In our follow-up, the median survival time is 39 months after surgery, ranging from 2 to 94 months. At the end of follow-up, 44 cases died. Statistical analyses were performed using SPSS 20.0 software (SPSS Inc., Chicago, IL, USA). Data was expressed as mean \pm standard deviations (SD). χ^2 test was used to assess the correlations between USP43 expression and clinicopathological characteristics. Student's t test or one-way ANOVA analysis was used to compare the differences between groups. P value less than 0.05 was considered to be statistically significant in all cases.

Results

Expression of USP43 in LUSC and its correlation with patients' characteristics

As shown in Fig. 1A, USP43 is predominately localized in the cytosol of LUSC cells, although it showed diverse expression levels in tissues from different patients. According to the immunoreactivity of IHC staining results, we grouped patients into low-USP43 (n = 81) and high-USP43 (n = 76) groups to assess their clinical correlations (Table 1). Chi-square tests showed that patients with larger tumor size were more prevalent to exhibit higher USP43 protein level (P = 0.020). Meanwhile, the expression level of USP43 was positively associated with patients' T stage (P < 0.001) and N stage (P = 0.006), respectively. The positive correlations between USP43 and unfavorable characteristics indicated that USP43 may participate in LUSC progression.

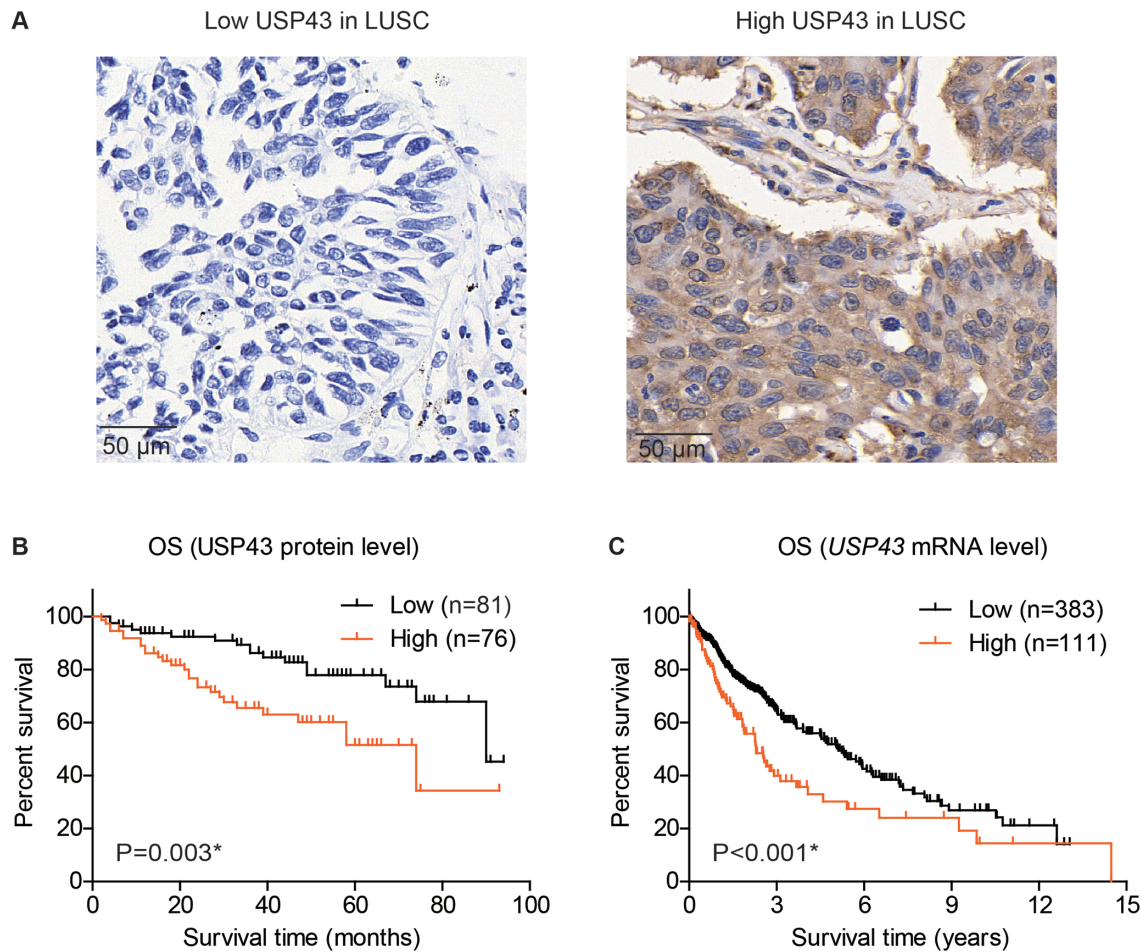


Fig. 1. Expression and prognostic role of USP43 in LUSC.

(A) Representative high- and low-expression of USP43 protein in LUSC tissues, as reflected by the immunohistochemical staining results. (B) Kaplan-Meier survival curve of the enrolled LUSC cohort from our medical center (n = 157), showing that patients with higher USP43 protein level exhibited poorer overall survival. (C) Kaplan-Meier survival curve of TCGA cohort (n = 494), showing that patients with higher USP43-mRNA level exhibited poorer overall survival.

*P < 0.05 by log-rank test.

Prognostic factors of LUSC patients

Kaplan-Meier method was utilized to assess the prognostic significance of USP43 protein in enrolled LUSC cohort (Fig. 1B). As a result, patients with higher USP43 showed shorter overall survival time (58.0 ± 5.1 months) compared to those with lower USP43 protein levels (76.5 ± 3.6 months). The 5-year overall survival rate of low-USP43 group was 77.8%, while it was only 51.6% of the high-USP43 group ($P = 0.003$). Considering that our data was

obtained from a single medical center with a limited case number, we next evaluated its prognostic role using TCGA cohort (Fig. 1C). Based on its mRNA levels from microarray data, we found that patients with higher USP43 transcription level also exhibited significant poorer overall survival compared to those with lower ones ($P < 0.001$). Taken together, either higher level of USP43-mRNA or USP43-protein was correlated with unfavorable prognosis of LUSC patients.

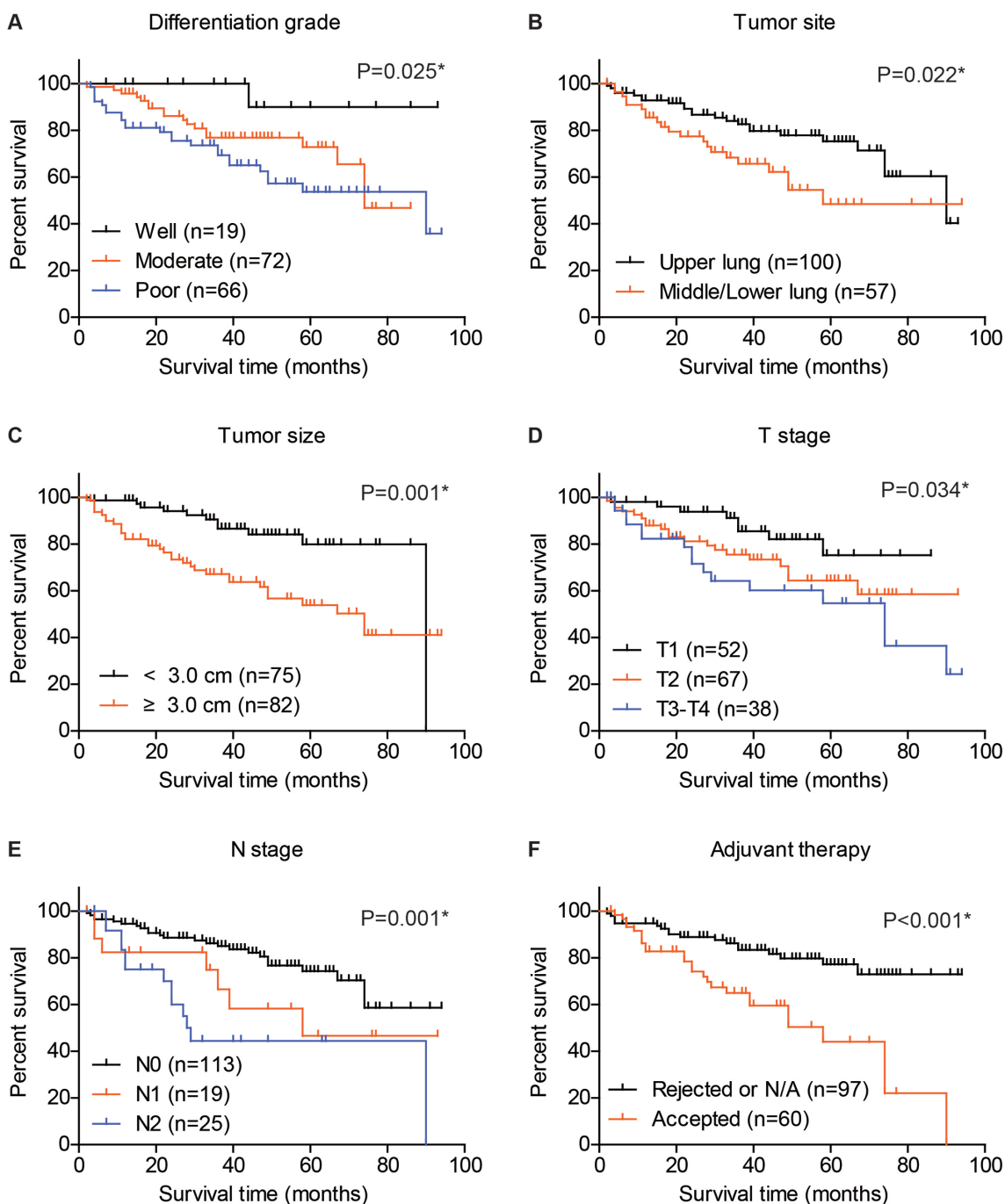


Fig. 2. Overall survival curves of enrolled 157 LUSC patients.

Kaplan-Meier survival curves were generated according to the LUSC differentiation grade (A), tumor site (B), tumor size (C), T stage (D), N stage (E), or adjuvant therapy (F). * $P < 0.05$ by log-rank test.

Table 2. Univariate analysis for the overall survival in 157 lung squamous cell carcinoma patients.

Variables	Cases (n = 157)	Overall survival (months)		P value
		Mean ± SEM	5-year OS rate	
Sex				0.271
Females	76	70.6 ± 4.0	67.6%	
Males	81	65.7 ± 4.3	64.1%	
Age				0.115
< 65 years	54	61.2 ± 5.4	46.4%	
≥ 65 years	103	72.1 ± 3.6	74.0%	
Differentiation grade				0.025*
Well	19	88.1 ± 4.6	90.0%	
Moderate	72	66.2 ± 3.8	72.8%	
Poor	66	62.0 ± 4.9	53.7%	
Tumor site				0.022*
Upper lung	100	73.0 ± 3.5	75.3%	
Middle/Lower lung	57	60.5 ± 5.5	48.4%	
Laterality				0.234
Left lung	70	64.9 ± 4.5	65.9%	
Right lung	87	72.4 ± 4.0	67.4%	
Tumor size				0.001*
< 3.0 cm	75	78.8 ± 3.4	79.9%	
≥ 3.0 cm	82	59.3 ± 4.4	53.9%	
T stage				0.034*
T1	52	73.9 ± 3.8	75.2%	
T2	67	67.4 ± 4.7	64.4%	
T3	38	59.7 ± 6.4	54.7%	
N stage				0.001*
N0	113	74.3 ± 3.4	74.3%	
N1	19	59.6 ± 9.3	46.6%	
N2	25	50.4 ± 8.1	44.4%	
Adjuvant therapy				< 0.001*
Rejected or unknown	97	77.6 ± 3.4	77.2%	
Accepted	60	52.6 ± 4.9	44.1%	
USP43 level				0.003*
Low	81	76.5 ± 3.6	77.8%	
High	76	58.0 ± 5.1	51.6%	

*Statistically significant by log-rank test.

USP43, ubiquitin specific peptidase 43; OS, overall survival.

Besides USP43 levels, the prognostic role of other enrolled factors was also analyzed using Kaplan-Meier method (Fig. 2, Table 2). Accordingly, poorer differentiation grade (Fig. 2A, $P = 0.025$), lower lung location of tumors (Fig. 2B, $P = 0.022$), larger tumor size (Fig. 2C, $P = 0.001$), advanced T stage (Fig. 2D, $P = 0.034$) and advanced N stage (Fig. 2E, $P = 0.001$) can all predict poorer overall survival of LUSC patients. Notably, patients accepted post-operative adjuvant therapies also exhibited poorer prognosis compared to those without adjuvant therapies (Fig. 2F, $P < 0.001$). This may be explained by the fact that only patients with advanced tumor stages were suggested for adjuvant therapy, which was significantly correlated with

poorer survival.

We next conducted multivariate analysis using a Cox regression model to evaluate their independent prognostic effects. All the factors showing statistical significance ($P < 0.05$) by univariate analyses in Table 2 were enrolled into the Cox regression model for multivariate analysis. In detail, the confounding factors included differentiation grade, tumor site, tumor size, T stage, N stage, adjuvant therapy, and USP43 expression (Table 3). As a result, high USP43 protein level was identified as an independent unfavorable prognostic biomarker of LUSC [hazard ratio (HR) 2.165, 95% confidence interval (CI) 1.064-4.408, $P = 0.033$]. Meanwhile, middle or lower lung tumor location

Table 3. Cox multivariate analysis for overall survival in 157 lung squamous cell carcinoma patients.

Variables	Hazard ratio	95% Confidence interval	P value
Differentiation grade			
Well	Reference		
Moderate	5.524	0.703-43.383	0.104
Poor	7.218	0.936-55.649	0.058
Tumor site			
Upper lung	Reference		
Middle/Lower lung	2.623	1.401-4.911	0.003*
Tumor size			
< 3.0 cm	Reference		
≥ 3.0 cm	2.891	1.142-7.319	0.025*
T stage			
T1	Reference		
T2	0.532	0.166-1.700	0.287
T3	0.415	0.112-1.540	0.189
N stage			
N0	Reference		
N1	1.406	0.562-3.521	0.467
N2	2.358	1.014-5.480	0.046*
Adjuvant therapy			
Rejected or unknown	Reference		
Accepted	1.913	0.848-4.318	0.118
USP43 level			
Low	Reference		
High	2.165	1.064-4.408	0.033*

*Statistically significant by Cox regression test.
USP43, Ubiquitin specific peptidase 43.

(HR 2.623, 95% CI 1.401-4.911, $P = 0.003$), larger tumor size (HR 2.891, 95% CI 1.142-7.319, $P = 0.025$), and stage N2 (HR 2.358, 95% CI 1.014-5.480, $P = 0.046$) all contributed independently to poorer overall survival of LUSC.

Considering the significant prediction efficiency of USP43 on LUSC survival, we further conducted stratification analyses based on T stage and N stage, respectively. As a result, high- or low-USP43 can help distinguish survival even in patients within the same T stage (Fig. 3A-C) or N stage (Fig. 3D, E). Therefore, we may conclude that monitoring USP43 expression level in LUSC tissues may help further predict patients' outcome as a supplement to the current TNM stage, which will help direct personalized follow-up.

USP43 knockdown inhibits LUSC proliferation and invasion

We next conducted cellular assays to validate the tumor-related role of USP43 in LUSC by knockdown strategy in NCI-H520 and NCI-H1703 cell lines (Fig. 4A-C). According to the CCK-8 assays, silencing USP43 can remarkably inhibited the proliferation capacity of both cell lines (Fig. 4D, E), which is consistent with the decreased

CDK1 level (Fig. 4A-C). Similarly, colony formation experiments also revealed an impaired cell growth upon USP43-knockdown (Fig. 4F, G).

Besides proliferation, we also tested whether USP43 has any effect on LUSC migration and invasion. As revealed by Transwell migration assays (Fig. 5A, B) and Matrigel-Transwell invasion assays (Fig. 5C, D), the cells treated with USP43-shRNAs exhibited significantly decreased migration and invasion capacities, comparing with the control cells. Therefore, we finally tested several well-known biomarkers that play roles in cell invasion, and found that both vimentin and snail can be positively regulated by USP43 (Fig. 4A-C). Taken together, our cellular data demonstrated that USP43 promotes LUSC progression by enhancing proliferation and invasion.

Discussion

In the current study, we investigated the expression of USP43 in LUSC for the first time. Based on our data, although USP43 exhibited distinct protein levels in tissues from different patients, higher USP43 was significantly correlated with aggressive tumor characteristics such as larger tumor size and advanced TNM stages. In the enrolled ret-

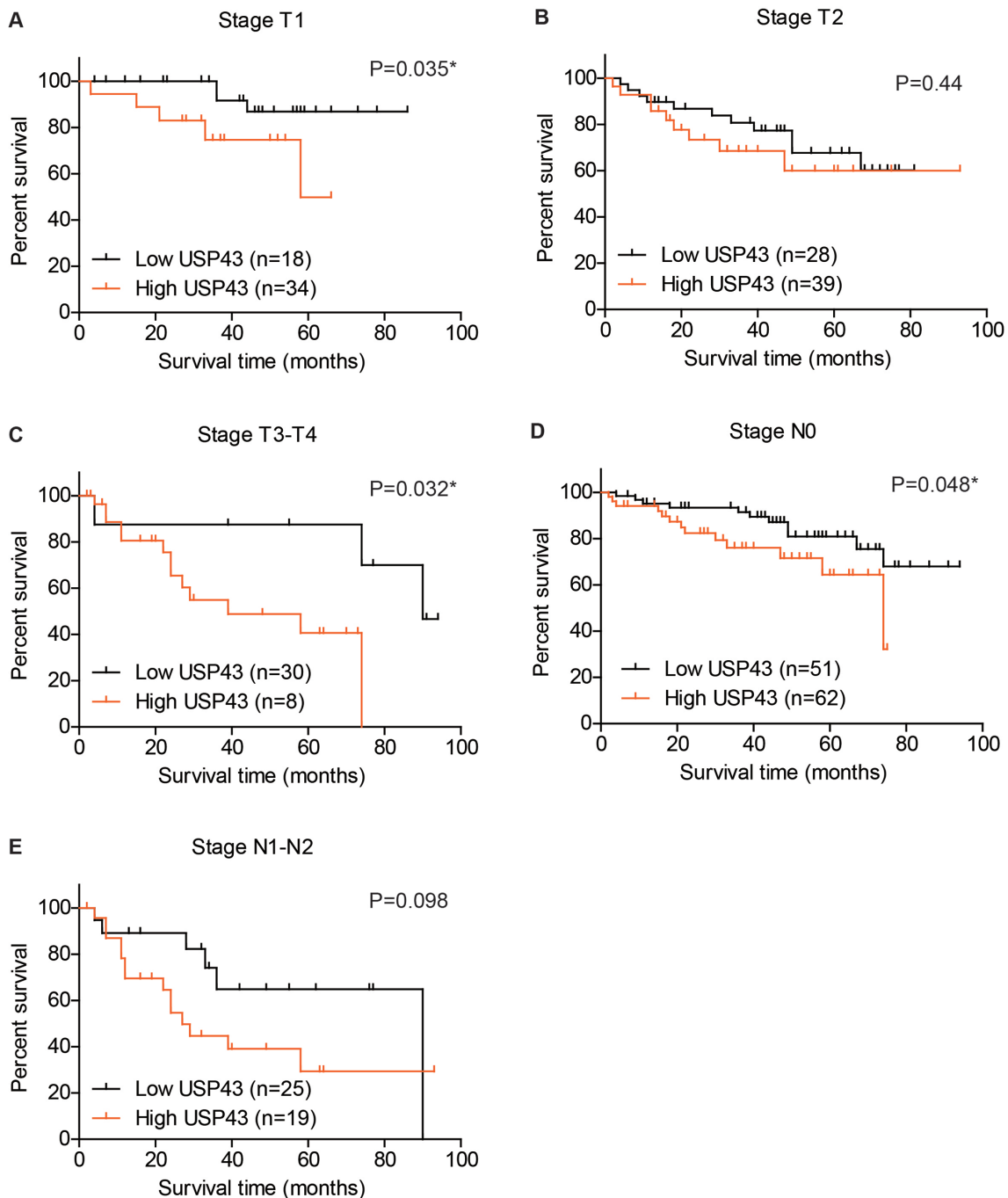


Fig. 3. Stratification survival analyses of 157 LUSC patients based on USP43 protein level.

The prognostic significance of USP43 protein expression level was evaluated in sub-grouped patients with stage T1 (A), stage T2 (B), stage T3-T4 (C), stage N0 (D), or stage N1-N2 (E). * $P < 0.05$ by log-rank test.

respective cohort, higher USP43 protein expression was also correlated with poorer overall survival of LUSC. Consistently, TCGA cohort also indicated that higher USP43 mRNA transcription can help predict unfavorable LUSC prognosis. Taken together with the multivariate data, we safely came to the conclusion that USP43 can serve as a novel independent prognostic factor to help predict LUSC survival.

Since clinical data revealed the significant positive

correlation between USP43 and tumor stages, we also conducted cellular assays to further validate its detailed effects in LUSC progression. Accordingly, silencing USP43 with specific shRNAs remarkably inhibited the proliferation and invasion processes of two LUSC cell lines. The effects of USP43 on LUSC growth and metastasis were consistent with its reported role in colorectal cancer and breast cancer (Lin et al. 2017; Ye et al. 2021). However, USP43 was a novel USP protein family member, only few studies

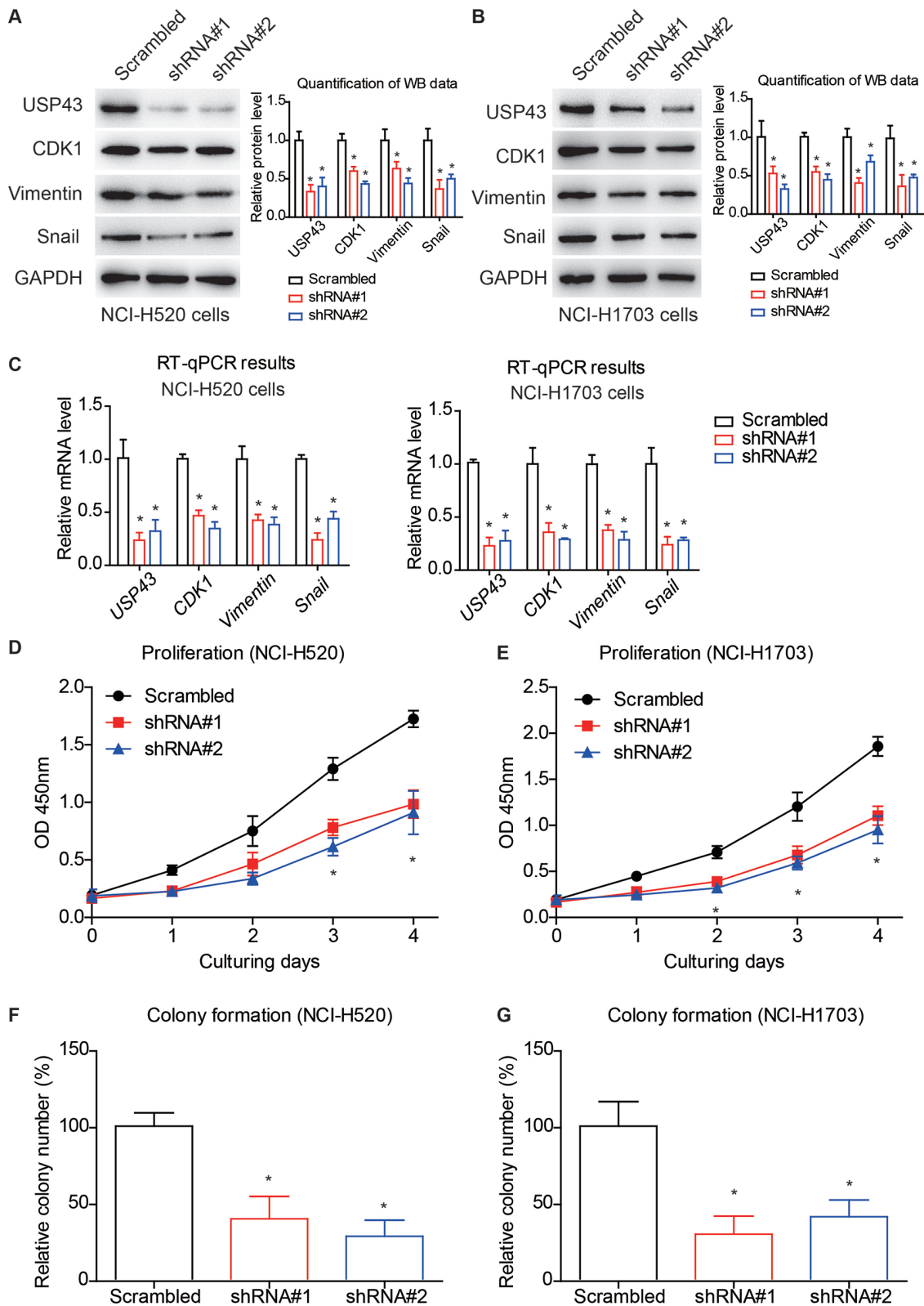


Fig. 4. Silencing USP43 inhibits LUSC cell proliferation.

(A, B) Western blotting analyses were conducted to test the knockdown efficiencies of shRNAs and the expression level of protein markers in NCI-H520 cells (A) and NCI-H1703 cells (B). (C) RT-qPCR assays were performed to assess the alterations of mRNA levels after knockdown in NCI-H520 and NCI-H1703 cells. (D, E) CCK-8 experiments revealed that silencing USP43 impaired the proliferation capacities of LUSC cell lines, NCI-H520 (D) and NCI-H1703 (E). (F, G) Colony formation also demonstrated the critical role of USP43 on maintaining cell proliferation of NCI-H520 cells (F) and NCI-H1703 cells (G). * $P < 0.05$ by Student's t-test compared with scrambled groups.

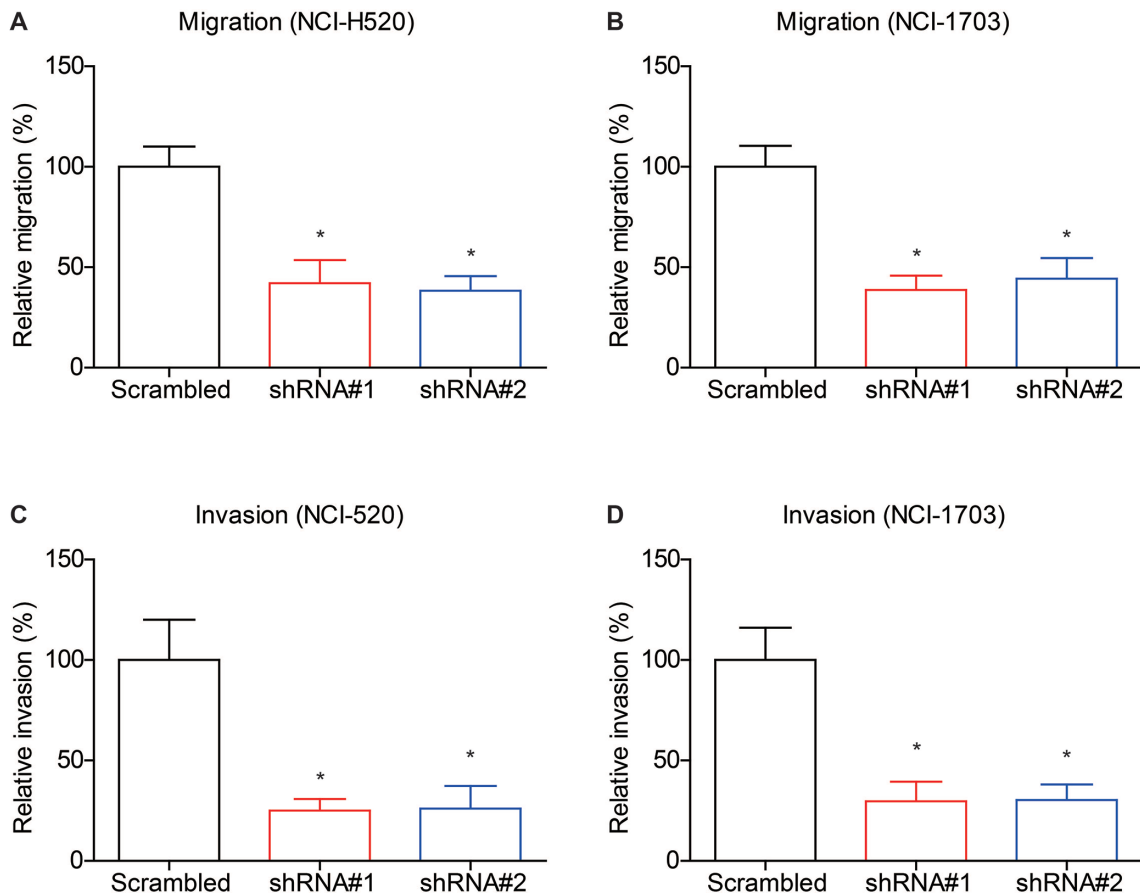


Fig. 5. USP43-knockdown results in decreased LUSC migration and invasion.

(A, B) Transwell assays were conducted to test the migration capacities of LUSC cell lines, NCI-H520 (A) and NCI-H1703 (B), which showed that silencing USP43 attenuated the cell migration. (C, D) Matrigel-Transwell experiments revealed that USP43-shRNA can significantly inhibit LUSC invasion in NCI-H520 cells (C) and NCI-H1703 cells (D).

* $P < 0.05$ by Student's t-test compared with scrambled groups.

reported its role in diseases. Here our data provided evidence that focusing on USP43 may be invaluable for therapeutic development.

To explore the downstream effectors of USP43, we next conducted immunoblotting assays to test the expression alteration of key regulators of proliferation and invasion. As a result, expression of CDK1, vimentin, and snail were all inhibited after silencing USP43, further confirming its oncogenic effects. Due to the equipment and technical limitations of the laboratory, we are currently unable to clarify the more detailed mechanism of USP43, such as its direct downstream substrates, which requires further research in the future (Zou et al. 2021). In addition, the combinational prognostic effect of USP43 and other biomarkers requires more clinical practice.

In conclusion, our study demonstrates the potential of USP43 as a novel prognostic biomarker for LUSC patients, and knockdown of USP43 exerts pivotal anti-cancer effects by inhibiting LUSC proliferation and invasion.

Author Contributions

Qingchao Sun conducted clinical analyses, Haiping

Zhang and Liang Zong performed cellular assays, Ainiwaer Julaiti helped collect clinical data, Xiaoliang Jing helped statistical analyses, Liwei Zhang designed this project.

Conflict of Interest

The authors declare no conflict of interest.

References

- Chen, J., Zou, Q. & Li, J. (2022) DeepM6ASeq-EL: prediction of human N6-methyladenosine (m6A) sites with LSTM and ensemble learning. *Front. Comput. Sci.*, **16**, 162302.
- Chen, L., He, M., Zhang, M., Sun, Q., Zeng, S., Zhao, H., Yang, H., Liu, M., Ren, S., Meng, X. & Xu, H. (2021a) The role of non-coding RNAs in colorectal cancer, with a focus on its autophagy. *Pharmacol. Ther.*, **226**, 107868.
- Chen, T., Liu, H., Liu, Z., Li, K., Qin, R., Wang, Y., Liu, J., Li, Z., Gao, Q., Pan, C., Yang, F., Zhao, W., Zhang, Z. & Xu, Y. (2021b) FGF19 and FGFR4 promotes the progression of gallbladder carcinoma in an autocrine pathway dependent on GPCR1-cAMP-EGR1 axis. *Oncogene*, **40**, 4941-4953.
- Gallo, L.H., Ko, J. & Donoghue, D.J. (2017) The importance of regulatory ubiquitination in cancer and metastasis. *Cell Cycle*, **16**, 634-648.
- He, L., Liu, X., Yang, J., Li, W., Liu, S., Liu, X., Yang, Z., Ren, J., Wang, Y., Shan, L., Guan, C., Pei, F., Lei, L., Zhang, Y., Yi, X.,

- et al. (2018) Imbalance of the reciprocally inhibitory loop between the ubiquitin-specific protease USP43 and EGFR/PI3K/AKT drives breast carcinogenesis. *Cell Res.*, **28**, 934-951.
- Lavaud, M., Mullard, M., Tesfaye, R., Amiaud, J., Legrand, M., Danieau, G., Brion, R., Morice, S., Regnier, L., Dupuy, M., Brounais-Le Royer, B., Lamoureux, F., Ory, B., Redini, F. & Verrecchia, F. (2021) Overexpression of the ubiquitin specific proteases USP43, USP41, USP27x and USP6 in osteosarcoma cell lines: inhibition of osteosarcoma tumor growth and lung metastasis development by the USP antagonist PR619. *Cells*, **10**, 2268.
- Li, J., D'Angiolella, V., Seeley, E.S., Kim, S., Kobayashi, T., Fu, W., Campos, E.I., Pagano, M. & Dynlacht, B.D. (2013) USP33 regulates centrosome biogenesis via deubiquitination of the centriolar protein CP110. *Nature*, **495**, 255-259.
- Lin, F., Xie, Z., Chang, L., Li, W., Wang, L., Hou, Y., Li, L., Zhu, J., Xia, Y., He, W. & Li, W. (2017) USP43 promotes tumorigenesis through regulating cell cycle and EMT in breast cancer. *Int. J. Clin. Exp. Pathol.*, **10**, 11014-11021.
- Liu, H., Gong, Z., Li, K., Zhang, Q., Xu, Z. & Xu, Y. (2021) SRPK1/2 and PP1alpha exert opposite functions by modulating SRSF1-guided MKNK2 alternative splicing in colon adenocarcinoma. *J. Exp. Clin. Cancer Res.*, **40**, 75.
- Liu, H., Wang, D., Zhang, Q., Zhao, Y., Mamonova, T., Wang, L., Zhang, C., Li, S., Friedman, P.A. & Xiao, K. (2019) Parallel post-translational modification scanning enhancing hydrogen-deuterium exchange-mass spectrometry coverage of key structural regions. *Anal. Chem.*, **91**, 6976-6980.
- Liu, H., Zhang, Q., Li, K., Gong, Z., Liu, Z., Xu, Y., Swaney, M.H., Xiao, K. & Chen, Y. (2016) Prognostic significance of USP33 in advanced colorectal cancer patients: new insights into beta-arrestin-dependent ERK signaling. *Oncotarget*, **7**, 81223-81240.
- Miller, K.D., Siegel, R.L., Lin, C.C., Mariotto, A.B., Kramer, J.L., Rowland, J.H., Stein, K.D., Alteri, R. & Jemal, A. (2016) Cancer treatment and survivorship statistics, 2016. *CA Cancer J. Clin.*, **66**, 271-289.
- Pal, A. & Donato, N.J. (2014) Ubiquitin-specific proteases as therapeutic targets for the treatment of breast cancer. *Breast Cancer Res.*, **16**, 461.
- Siegel, R.L., Miller, K.D. & Jemal, A. (2020) Cancer statistics, 2020. *CA Cancer J. Clin.*, **70**, 7-30.
- Tang, W., Wan, S., Yang, Z., Teschendorff, A.E. & Zou, Q. (2018) Tumor origin detection with tissue-specific miRNA and DNA methylation markers. *Bioinformatics*, **34**, 398-406.
- Tian, Z., D'Arcy, P., Wang, X., Ray, A., Tai, Y.T., Hu, Y., Carrasco, R.D., Richardson, P., Linder, S., Chauhan, D. & Anderson, K.C. (2014) A novel small molecule inhibitor of deubiquitylating enzyme USP14 and UCHL5 induces apoptosis in multiple myeloma and overcomes bortezomib resistance. *Blood*, **123**, 706-716.
- Wang, S.A., Wang, Y.C., Chuang, Y.P., Huang, Y.H., Su, W.C., Chang, W.C. & Hung, J.J. (2017) EGF-mediated inhibition of ubiquitin-specific peptidase 24 expression has a crucial role in tumorigenesis. *Oncogene*, **36**, 2930-2945.
- Wang, Y. & Wang, F. (2021) Post-translational modifications of deubiquitinating enzymes: expanding the ubiquitin code. *Front. Pharmacol.*, **12**, 685011.
- Wang, Y.C., Wu, Y.S., Hung, C.Y., Wang, S.A., Young, M.J., Hsu, T.I. & Hung, J.J. (2018) USP24 induces IL-6 in tumor-associated microenvironment by stabilizing p300 and beta-TrCP and promotes cancer malignancy. *Nat. Commun.*, **9**, 3996.
- Xu, Y.F., Liu, H.D., Liu, Z.L., Pan, C., Yang, X.Q., Ning, S.L., Zhang, Z.L., Guo, S. & Yu, J.M. (2018) Sprouty2 suppresses progression and correlates to favourable prognosis of intrahepatic cholangiocarcinoma via antagonizing FGFR2 signalling. *J. Cell. Mol. Med.*, **22**, 5596-5606.
- Yan, S., Yan, J., Liu, D., Li, X., Kang, Q., You, W., Zhang, J., Wang, L., Tian, Z., Lu, W., Liu, W. & He, W. (2021) A nanopredator of pathological MDMX construct by clearable supra-molecular gold(I)-thiol-peptide complexes achieves safe and potent anti-tumor activity. *Theranostics*, **11**, 6833-6846.
- Ye, D.X., Wang, S.S., Huang, Y., Wang, X.J. & Chi, P. (2021) USP43 directly regulates ZEB1 protein, mediating proliferation and metastasis of colorectal cancer. *J. Cancer*, **12**, 404-416.
- Young, M.J., Hsu, K.C., Lin, T.E., Chang, W.C. & Hung, J.J. (2019) The role of ubiquitin-specific peptidases in cancer progression. *J. Biomed. Sci.*, **26**, 42.
- Zhang, Q., Fan, H., Liu, H., Jin, J., Zhu, S., Zhou, L., Liu, H., Zhang, F., Zhan, P., Lv, T. & Song, Y. (2020) WNT5B exerts oncogenic effects and is negatively regulated by miR-5587-3p in lung adenocarcinoma progression. *Oncogene*, **39**, 1484-1497.
- Zhang, Q., Fan, H., Zou, Q., Liu, H., Wan, B., Zhu, S., Hu, Y., Li, H., Zhang, C., Zhou, L., Zhu, Q., Xiao, K., Zhang, J., Zhan, P., Lv, T., et al. (2018a) TEAD4 exerts pro-metastatic effects and is negatively regulated by miR6839-3p in lung adenocarcinoma progression. *J. Cell. Mol. Med.*, **22**, 3560-3571.
- Zhang, Q., Hu, H., Liu, H., Jin, J., Zhu, P., Wang, S., Shen, K., Hu, Y., Li, Z., Zhan, P., Zhu, S., Fan, H., Zhang, J., Lv, T. & Song, Y. (2018b) RNA sequencing enables systematic identification of platelet transcriptomic alterations in NSCLC patients. *Biomed. Pharmacother.*, **105**, 204-214.
- Zhang, Q., Liu, H., Zhu, Q., Zhan, P., Zhu, S., Zhang, J., Lv, T. & Song, Y. (2017) Patterns and functional implications of platelets upon tumor "education". *Int. J. Biochem. Cell Biol.*, **90**, 68-80.
- Zou, Q., Xing, P., Wei, L. & Liu, B. (2019) Gene2vec: gene subsequence embedding for prediction of mammalian N (6)-methyladenosine sites from mRNA. *RNA*, **25**, 205-218.
- Zou, Y., Wu, H., Guo, X., Peng, L., Ding, Y., Tang, J. & Guo, F. (2021) MK-FSVM-SVDD: a multiple kernel-based fuzzy SVM model for predicting DNA-binding proteins via support vector data description. *Curr. Bioinform.*, **16**, 274-283.